Distinct Ion Channel Classes Are Expressed on the Outer Nuclear Envelope of T- and B-Lymphocyte Cell Lines

Alfredo Franco-Obregón,* Hong-wei Wang,† and David E. Clapham†

*Solid State Physics Laboratory, ETH Zurich, CH 8093 Zurich, Switzerland, and †Department of Basic Cardiovascular Research, Howard Hughes Medical Institute, Children's Hospital/Harvard Medical School, Boston, Massachusetts 02115 USA

ABSTRACT The outer nuclear membrane, endoplasmic reticulum, and mitochondrial membrane ion channels are poorly understood, although they are important in the control of compartmental calcium levels, cell division, and apoptosis. Few direct recordings of these ion channels have been made because of the difficulty of accessing these intracellular membranes. Using patch-clamp techniques on isolated nuclei, we measured distinct ion channel classes on the outer nuclear envelope of T-cell (human Jurkat) and BFL5 cell (murine promyelocyte) lines. We first imaged the nuclear envelopes of both Jurkat and FL5 cells with atomic force microscopy to determine the density of pore proteins. The nuclear pore complex was intact at roughly similar densities in both cell types. In patch-clamp recordings of Jurkat nuclear membranes, Cl channels (105 ± 5 pS) predominated and inactivated with negative pipette potentials. Nucleotides transiently inhibited the anion channel. In contrast, FL5 nuclear channels were cation selective (52 ± 2 pS), were inactivated with positive membrane potentials, and were insensitive to GTPγS applied to the bath. We hypothesize that T- and B-cell nuclear membrane channels are distinct, and that this is perhaps related to their unique roles in the immune system.

INTRODUCTION

The nuclear envelope functionally separates nucleoplasmic from cytoplasmic compartments. Communication between these two compartments is mediated through the nuclear pore complex, a macromolecular structure spanning the inner and outer leaflets of the nuclear envelope and comprising 100–200 different polypeptides (Gorlich, 1988; Weis, 1998). Bidirectional active transport of larger macromolecules (>60 kDa) and nucleic acids through the nuclear pore complex requires directionally specified localization sequences (nuclear or cytoplasmic) and is catalyzed by nuclear importer and exporter GTPases. Smaller macromolecules and ions, on the other hand, are thought to freely diffuse through the nuclear pore complex, as evidenced by the fact that Ca^{2+} increments initiated in the cytosol rapidly diffuse into the nuclear compartment (Stehno-Bittel et al., 1995b; Lipp et al., 1997; Perez-Terzic et al., 1997).

The area between the inner and outer nuclear envelope defines the perinuclear space (or cisternae), which in combination with the lumen of the endoplasmic reticulum, creates a continuous, interconnected network that serves as a reservoir for intracellular calcium (reviewed by Petersen et al., 1998; Clapham, 1995). The outer nuclear envelope can be envisioned as an extension of the endoplasmic reticular membrane. Both the outer nuclear and endoplasmic reticulum membranes possess Ca^{2+} ATPases (SERCA pumps) and $InsP_3$ receptors that regulate cisternal Ca^{2+} concentrations (Lanini et al., 1992; Humbert et al., 1996; Stehno-Bittel et al., 1995a). In contrast, the inner nuclear envelope's protein composition is distinct from that of the outer envelope (Gilchrist and Pierce, 1993; Humbert et al., 1996).

Although the nuclear envelope and endoplasmic reticulum have been shown to be functionally interconnected (Subramanian and Meyer, 1997), they may also act like independent Ca^{2+} release sites (reviewed by Petersen et al., 1998). For example, Ca^{2+} is selectively mobilized into the nucleoplasmic compartment as the result of the opening of $InsP_3$-gated channels on the inner nuclear envelope (Gerasimenko et al., 1995; Hennager et al., 1995). Furthermore, the biosynthetic machinery for the production of $InsP_3$ is found within the nucleus (reviewed by Divecha et al., 1993). Cyclic ADP-ribose (ryanodine)-sensitive Ca^{2+}-release channels may similarly mediate nuclear-specific Ca^{2+} signals (Gerasimenko et al., 1995; Guihard et al., 1997). Ligand-gated Ca^{2+} release channels are therefore a common feature of the nuclear envelope and endoplasmic reticulum (see also Stehno-Bittel et al., 1995a,b).

It is increasingly evident that other classes of ion channels also perform unknown functions in these intracellular compartments (Al-Awqati, 1995). For example, some members of the ubiquitous double-barreled chloride channel family, or ClCs, are thought to function intracellularly. ClC-6 colocalizes with the SERCA 2b pump of the endoplasmic reticulum, where it is proposed to dissipate the electrical gradient created by the movement of Ca^{2+} into the lumen of the endoplasmic reticulum (Brandt and Jentsch, 1995; cf. Buyse et al., 1997, 1998). Chloride influx via ClC-6 would thereby balance the excess positive charge from the loading of Ca^{2+} into the endoplasmic reticulum. This notion is further supported by the finding that the anion channel blockers, NPPB and R(+)-IAA-94, preclude Ca^{2+}

Received for publication 3 November 1999 and in final form 16 March 2000.

Address reprint requests to Dr. David E. Clapham, Howard Hughes Medical Institute, Children's Hospital/Harvard Medical School, Room 1309, Ender's Building, P.O. Box EN-306, 320 Longwood Avenue, Boston, MA 02115. Tel.: 617-355-6163; Fax: 617-731-0787; E-mail: clapham@rascal.med.harvard.edu.

0006-3495/00/07/202/13 $2.00

uptake into the sarcoplasmic reticulum of gastric smooth muscle (Pollock et al., 1998). These same channel blockers also inhibit chloride channel activity from brain endoplasmic reticulum in artificial bilayers (Clark et al., 1997). Finally, the existence of ClC channels on the endoplasmic reticulum has been functionally demonstrated in artificial bilayers (Morier and Sauve, 1994). Taken together, these studies suggest that luminal Ca^{2+} loading is dependent on the activity of intracellular ClC channels. The fact that depletion of the perinuclear calcium stores halts diffusion of molecules smaller than than ~60 kDa through the nuclear pore complex may also implicate intracellular ClC channels in nuclear trafficking (reviewed by Perez-Terzic et al., 1997).

Intracellular ion channels have been recorded in artificial lipid bilayers fused with membrane vesicles derived from nuclear envelopes (cationic and anionic; Rousseau et al., 1996) and the endoplasmic reticulum (anionic; Clark et al., 1997; Eliassi et al., 1997). They have been directly demonstrated in single-channel recordings from intact nuclei (Mazzanti et al., 1990, 1998). Valenzuela et al. (1997) recently cloned an anion channel homolog from nuclear membranes (p64). In addition to its nuclear localization, p64 appears on the plasma membrane when overexpressed in CHO-K1 cells and has a single-channel conductance of 22 pS. Other p64 homologs have also been cloned from brain endoplasmic reticulum (43 pS; Duncan et al., 1997) as well as kidney microsomes (42 pS; Landry et al., 1993; Edwards et al., 1998).

In this report we functionally characterize the ion channels expressed on the nuclear envelope of hematopoietic cell lines. Surprisingly, the nuclear envelopes of Jurkat (T lymphocytes) and FL5 (pro B lymphocytes) cell lines express distinct classes of ion channels. Jurkat nuclei express anion channels with single-channel conductances of ~80 pS, while FL5 cells primarily express a cation-selective channel of ~50 pS. A preliminary version of this work appeared as an abstract (Franco-Obregón and Clapham, 1998).

EXPERIMENTAL PROCEDURES

Cell culture

Jurkat and FL5 cells were obtained from Dr. Craig B. Thompson (Howard Hughes Medical Institute, University of Chicago). Jurkats were grown in RPMI 1640 (Gibco BRL) supplemented with 10% fetal calf serum and 10 mM HEPES (Gibco BRL). FL5 cells were grown in basic Jurkat medium that had been further supplemented with β-mercaptoethanol (2 μl/500 ml) and 10% WEH1–3B supernatant. Supernatant was harvested from WEH1–3B cells that had been grown in FL5 medium. Aliquots of WEHI-3B supernatant (50 ml) were kept at −20°C until use. Intact nuclei were isolated after swelling and homogenized in hypotonic medium. Approximately 1×10^6 cells/ml were centrifuged at 400 × *g* for 5 min, and the resulting pellet was resuspended in hypotonic medium (55 mmol/kg) composed of (in mM) 10 KCl, 1.5 $MgCl_2$, 10 HEPES free acid, and 0.5 D,L-dithiothreitol (pH 7.9). Cells were then incubated on ice for 10 min, followed by centrifugation at 400 × *g* for 3 min. The cell pellet was resuspended in 5–7 ml of ice-cold hypotonic medium and homogenized with 10 strokes of a large clearance pestle in a Dounce homogenizer. The cell homogenate was then spun at 400 × *g* for 3 min, and the supernatant containing extranuclear material was discarded. The nuclear pellet was washed twice (spun at 400 × *g* for 1 min) and resuspended in storage medium consisting of (in mM) 140 KCl, 2 $MgCl_2$, 0.1 $CaCl_2$, 5 glucose, 1.1 EGTA, and 10 HEPES free acid (pH 7.3) in preparation for single-channel recording. The nuclei were stored at 4°C until use.

Electrophysiology

Single-channel recordings were made on isolated nuclei, using an Axopatch 200B integrating patch-clamp amplifier (Axon Instruments). Data were filtered at 5 kHz and stored on videotape. For off-line analysis, current records were digitized through a DigiData 1200 A-D converter, using pClamp6 software (Axon Instruments), and stored on disk. Patch recording electrodes were filled with a solution consisting of (in mM) 150 KCl, 5 $MgCl_2$, 10 HEPES free acid (pH 7.4). The bathing solutions consisted of either (in mM) 150 K-aspartate or 150 K-gluconate in addition to 5 $MgCl_2$, 5 EGTA, and 10 HEPES free acid (pH 7.4). The osmolarity of all recording solutions was adjusted to within 290–305 mmol/kg before use. The bath was perfused by gravity, and complete exchange of the bath volume (200 μl) required ~10 s. Continual perfusion of the bath or changing the bath composition had no effect on the liquid junction potential. After fire polishing, patch electrodes had a resistance of 3.5 ± 0.5 MΩ (± SD, $n = 68$). All recordings were conducted at room temperature (22 ± 2°C). An agar bridge was utilized as a ground electrode. Changing the bath composition did not result in changes in liquid junction potential. Inward (negative) currents are depicted as downward current deflections resulting from the flow of anions out of the recording pipette or cations flowing into the recording pipette (see Fig. 1).

Atomic force microscopy

Atomic force microscopy was performed on intact nuclei prepared in the same manner as for electrophysiology, with the exception that after homogenization the nuclei were resuspended in normal nuclear storage medium containing fixatives (4% formaldehyde and 1% glutaraldehyde). One hour after fixation the nuclei were transferred to poly-L-lysine-coated coverslips (5%; Sigma) and allowed to adhere at room temperature. The nuclei were then rinsed twice with double-distilled water and allowed to dry. The nuclei surface was imaged using a BioScope (NanoScope IIIa; Digital Instruments, Santa Barbara, CA) mounted on an inverted optical microscope with standard single-beam silicon cantilevers of length 125 μm (spring constant 0.06 N/m). Cantilever tips had an estimated diameter of ~5–10 μm. Surface images of nuclei were obtained in tapping mode in air with a typical scan rate of 1 Hz.

Confocal microscopy

Confocal microscopy was performed with a laser scanning microscope (LSM 410; Carl Zeiss). In preparation for confocal imaging, FL5 nuclei were prepared in the same manner as for electrophysiology, with the exception that after dissociation they were placed in a bathing solution consisting of (in mM) 140 KCl, 10 HEPES, and 5 $MgCl_2$. Nuclear envelopes were loaded with 10 μM Oregon Green 488 BAPTA-5N (Molecular Probes, Eugene, OR), a low-affinity Ca^{2+} indicator, for 30 min at 37°C. Oregon Green 488 BAPTA-5N is reported to have a K_d for Ca^{2+} binding of ~20 μM in the absence of Mg^{2+} (Molecular Probes Handbook, 6th edition). The solution was adjusted to pH 7.2. The nuclei were excited with the 488-nm line of a krypton/argon laser, and emission was collected at 523 nm.

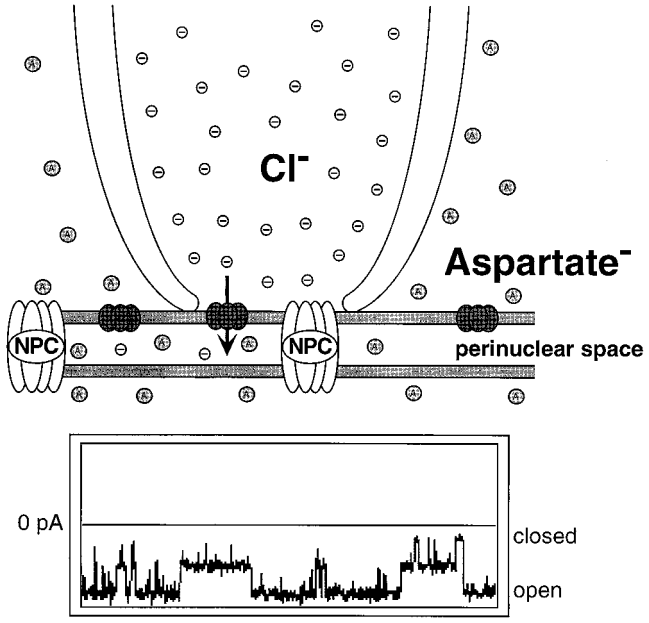

FIGURE 1 Schematic representation of the recording configuration with 150 mM KCl in the electrode and 150 mM K-aspartate in the bath (also referred to in the text as "extranuclear"). The smaller (*open*) and larger (*shaded*) circles represent chloride and aspartate anions, respectively. The cationic counterion (K^+) is not shown in the figure for clarity. The nuclear pore complex (NPC) spans the entire perinuclear space. The Jurkat anion channel is depicted as the shaded multimeric complex spanning only the outer nuclear envelope. The perinuclear space (nuclear cisterna) is presumed to be completely dialyzed via the bath. The flow of Cl^- out of the patch electrode (*arrow*) is seen as an inward current (downward openings), as shown in the current records at the bottom of the figure. The opposite would be true for cations: the flow of K^+ into the electrode would also be perceived as an inward current. In this respect a negative patch pipette potential would induce inward currents by both anions and cations. The drawing shows one anion channel and one nuclear pore (not drawn to scale).

RESULTS

Atomic force microscopic images of isolated nuclei from Jurkat and FL5 cells

The aim of this study was to examine ion channel activity originating from the nuclear envelope of distinct hematopoietic cell types. To reduce the possibility that our recordings were made from remnants of the endoplasmic reticulum rather than the nuclear envelope, it was necessary to visualize the surface features of dissociated nuclei. Fig. 2 shows surface images of dissociated nuclei from Jurkat (*left*) and FL5 (*right*) cells. Fig. 2, *A* and *C–F*, were obtained with the atomic force microscope and confirmed the integrity of the outer nuclear envelope, as evidenced by the presence of the nuclear pore complex. Since Fig. 2 *A* represents an area of nuclear envelope roughly equivalent to that contained within a typical patch electrode (2–4-μm diameter), more than 50 nuclear pores should have been present within each on-nucleus patch recording. The densities of nuclear pores for Jurkat and FL5 nuclei were $14 \pm 10/\mu m^2$ ($\pm$ SD; $n = 16$) and $40 \pm 19/\mu m^2$ ($\pm$ SD; $n = 13$), respectively. Our results agree reasonably well with previous estimates of nuclear pore density ($3.3/\mu m^2$, Mazzanti et al., 1990; $20–30/\mu m^2$, Mazzanti et al., 1994; $1–50/\mu m^2$, Perez-Terzic et al., 1997; $13/\mu m^2$, Tonini et al., 1999; $\sim 46/\mu m^2$, Wang and Clapham, 1999). Despite this fact, we rarely saw channel openings representing a conductance greater than 1 nS, a size previously estimated to pass through the open nuclear pore (Mazzanti et al., 1990). We conclude that the nuclear pores were not conducting under our recording conditions (see Discussion).

On occasion, the presence of attached endoplasmic reticular membrane could be observed on the outer periphery of isolated nuclei (see also Danker et al., 1997). Fig. 2 *B* is a confocal microscope image of a dissociated nucleus demonstrating remnants of the endoplasmic reticulum still attached to the nuclear envelope. Although it is possible, it is unlikely that the channel activity we measured arose from the endoplasmic reticulum. Endoplasmic reticulum membranes were too disrupted and rare to account for the high success rate (60–90%) in gigaseal formation of the on-nucleus recordings. The ion channel activity described in this report most likely originated from the nuclear envelope.

One key assumption in our studies and others is that the bath solution had free access to the intranuclear space. This assumption was verified, inasmuch as the intranuclear space was readily filled with Oregon Green after bath perfusion. The tight clustering of the conductance and reversal potential values, indicating negligible voltage offsets, can again be taken as evidence for the low resistance access to the intracisternal compartment via the bath. Finally, channel measurements were not influenced by patch excision from the nuclear envelope, indicating that the ion concentrations in the bath and cisternal solutions were the same.

Anion selectivity of nuclear channels in Jurkat nuclei

Previous accounts of ion channel activity from the outer nuclear envelope have described both cation- and anion-permeable channels (for reviews see Stehno-Bittel et al., 1996; Mazzanti, 1998). We therefore established recording conditions that would unequivocally identify the cation or anion selectivity of channel types while permitting the recording of both channel types. Under our standard recording conditions consisting of 150 mM K-aspartate in the bath and 150 mM KCl in the electrode, the reversal potentials for chloride and potassium were widely separated ($\sim +70$ mV and 0 mV, respectively). Representative examples of current traces obtained from Jurkat nuclei are shown in Fig. 3 in the presence of a symmetrical chloride gradient (Fig. 3 *A*) and under our standard conditions (Fig. 3 *B*). With 150 mM KCl in the recording electrode and bath (symmetrical chloride; Fig. 3 *A*), both inward (-60 mV) and outward ($+60$

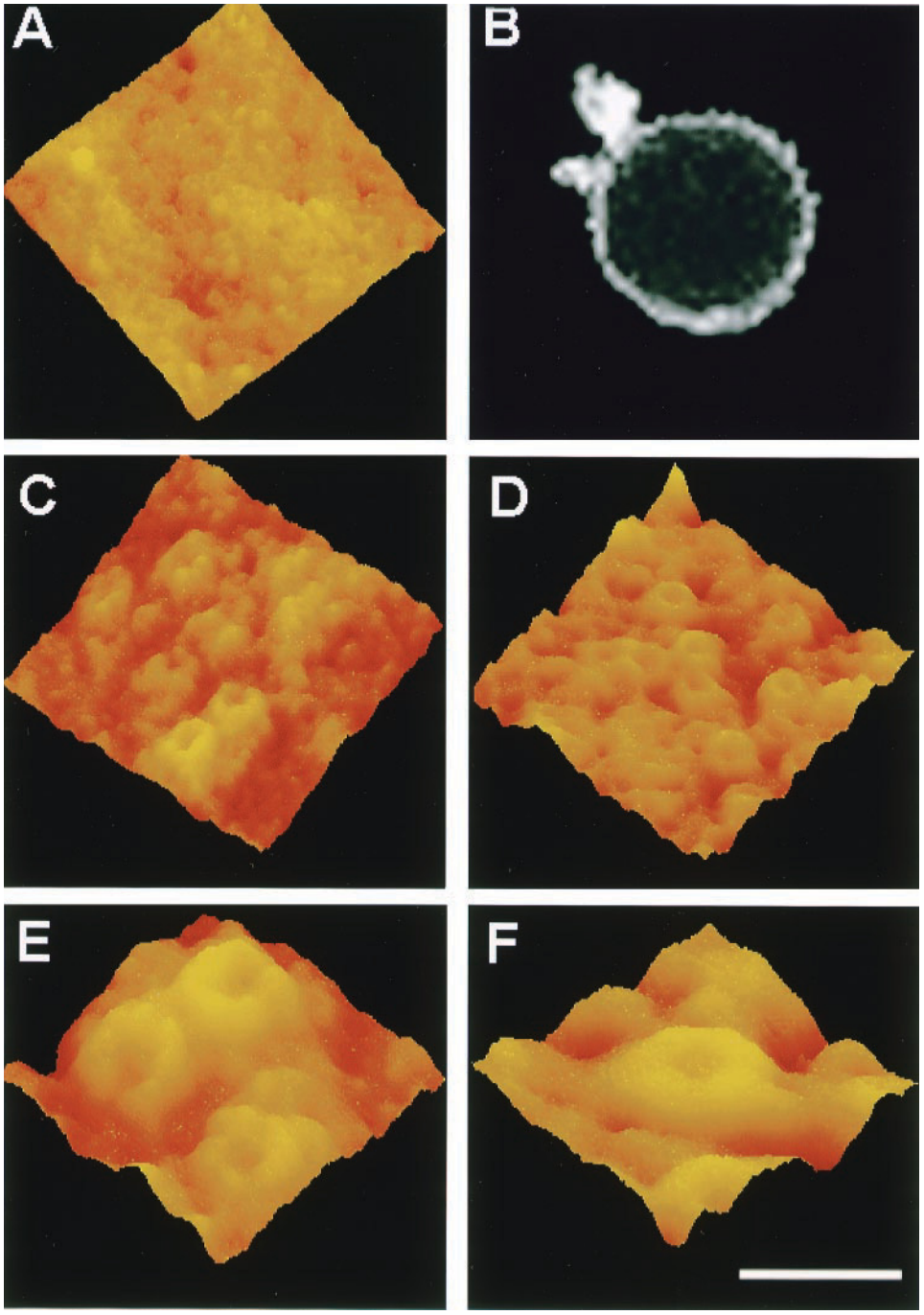

FIGURE 2 Surface images of isolated nuclei from Jurkat (*A, C,* and *E*) and FL5 (*B, D,* and *F*) cells. (*A, C–E*) Atomic force microscope images of dissociated nuclei displayed at different magnifications. The scale bar in *F* represents 1 μm for *A*, 350 nm and 400 nm for *C* and *D*, respectively, and 167 and 137 nm for *E* and *F*, respectively. (*B*) Unfixed dissociated FL5 nucleus loaded with Oregon Green 488 BAPTA-5N in 2 mM Ca^{2+} external solution and imaged by confocal microscopy. Note the presence of an intact perinuclear space and remnants of the endoplasmic reticulum membrane attached to the nuclear envelope. The scale bar in *F* represents 6 μm for *B*.

mV) currents were clearly resolved. Replacing bath chloride with aspartate greatly reduced or abolished the outward currents (Fig. 3 *B*). Fig. 3, *C* and *D*, shows the single-channel current-voltage relationships obtained from two recordings in the presence of symmetrical KCl and after replacing KCl in the bath with either K-aspartate (Fig. 3 *C*) or K-gluconate (Fig. 3 *D*). In the presence of symmetrical KCl, the current-voltage relationships for both recordings inwardly rectified and single-channel currents reversed at 0 mV (*empty circles*). Replacing bath chloride with either aspartate or gluconate precluded the outward currents and shifted the reversal potentials positively by 22 $\pm$ 0.7 mV ($\pm$ SEM; $n = 5$; *filled circles*). Furthermore, the rectification of the current-voltage relationship persisted in the presence of symmetrical KCl, indicating that it is an inherent property of the channel and not the result of unidirectional anion flux. For these recordings, the inward single-channel slope conductances in the presence of symmetrical KCl were 108 pS (Fig. 3 *C*) and 101 pS (Fig. 3 *D*) between -60 mV and -80 mV. Channel conductances were smaller when aspartate or

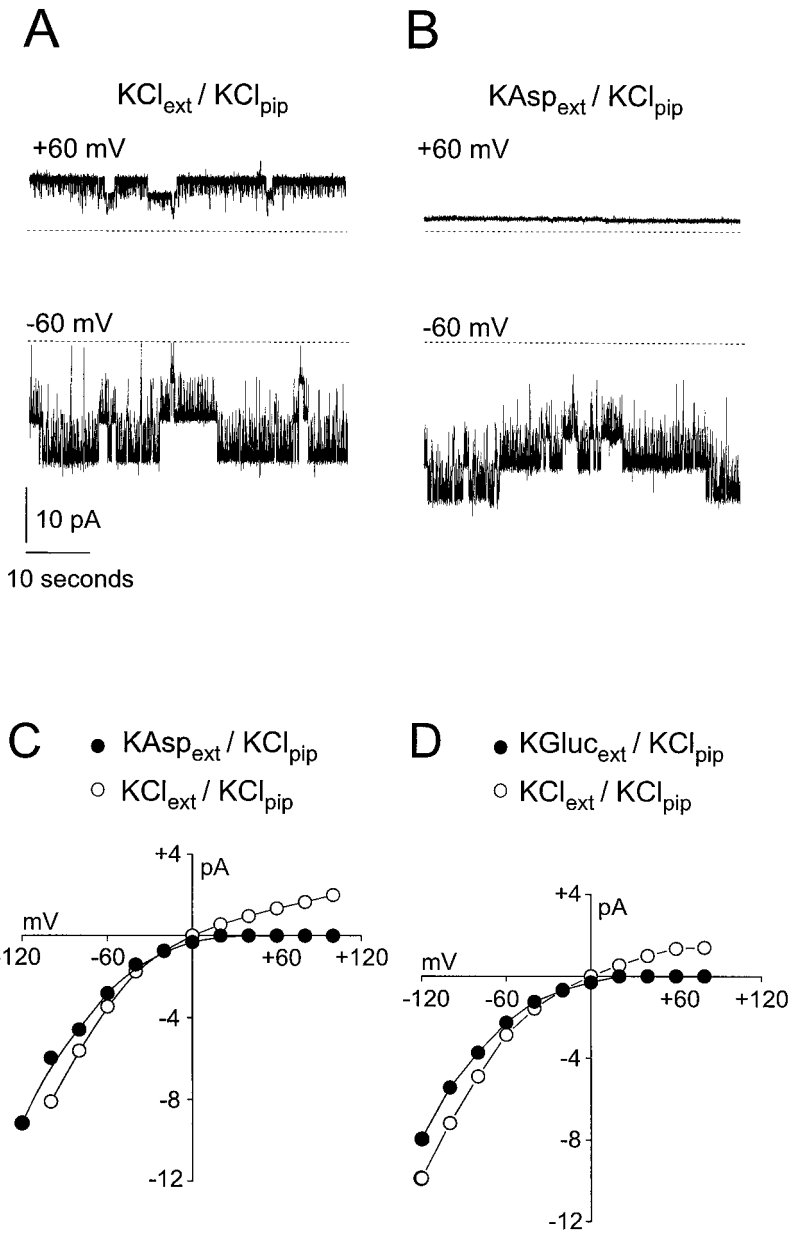

FIGURE 3 Chloride channel activity recorded from the surface of Jurkat nuclei. (*A* and *B*) Single-channel currents obtained at the indicated patch potentials in the presence of symmetrical KCl (*A*) or with extranuclear K-aspartate (*B*). The dashed lines indicate the 0 current level. Chloride conduction is apparent from the appearance of outward currents in the presence of symmetrical KCl. The mean inward slope conductance for such channels with extranuclear K-aspartate was 82 ± 3 pS (± SEM; $n = 9$). (*C* and *D*) Single-channel current-voltage relationships obtained with 150 mM KCl in the recording pipette and 150 mM of either KCl (○, *C* (108 pS) and *D* (101 pS)), K-aspartate (●, *C* (85 pS)), or K-gluconate (●, *D* (74 pS)) in the bath. Inward slope conductances were calculated between the pipette potentials of −40 and −80 mV. Subsequently excising the patch from the nuclear surface did not alter single-channel conductance or reversal potentials. In this and subsequent figures KCl_{pip} and KCl_{ext} refer to the presence of 150 mM KCl in the recording pipette or the extranuclear bath, respectively (see Experimental Procedures). Likewise, KAsp and KGluc refer to the 150 mM K-aspartate and 150 K-gluconate bathing solutions, respectively. Traces were filtered at 500 Hz and sampled at 2 kHz.

gluconate replaced chloride in the bath (85 pS (Fig. 3 *C*) and 74 pS (Fig. 3 *D*), respectively). Channel conductance fully reverted when the bath was reperfused with 150 mM chloride (data not shown). The mean slope conductance for several recordings with K-aspartate in the bath and KCl in the electrode was 82 ± 3 pS (± SEM; $n = 9$). Such channels were observed in 13 of 15 on-nucleus patches from recordings of Jurkat nuclei. Other anion channel classes were observed in the remaining recordings. Finally, channel activity was completely abolished in the presence of symmetrical K-aspartate, demonstrating the absence of a cation conductance. In summary, the channels recorded from Jurkat nuclei were anion selective and were active under native conditions.

Anion channel open probability was typically high in Jurkat nuclear recordings. Although channel openings overlapped too often to easily assess channel kinetics, the mean open time at −100 mV was ~50 ms. Lowering the pH of the pipette solution to from 7.4 to 4.0 greatly reduced channel activity, which suggests that channel gating is altered by protonation of the channel. On occasions when channel activity was sufficiently low we could detect double-barreled gating, as previously described for other ClC channels (e.g., Miller and White, 1984). Fig. 4 shows opening transitions from intermediate to double-conductance levels. As is characteristic of double-barreled gating, we never detected more than two subconductance levels, and the intermediate conductance level was exactly half that of

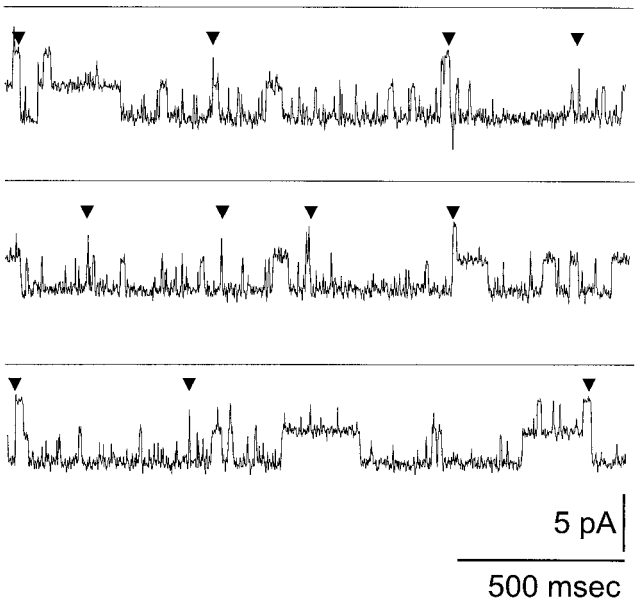

FIGURE 4 Double-barreled gating of Jurkat anion channel. Examples of current records displayed double-barrel openings indicated by the arrows. The pipette potential was −60 mV. The current records were filtered at 1 kHz and sampled at 5 kHz. The conductance of the first level was 94 pS with K-aspartate in the bath.

the fully open channel. Similar, anion-selective, double-conductance openings have previously been demonstrated in vesicles derived from the outer nuclear envelope (Rousseau et al., 1996) and endoplasmic reticulum vesicles incorporated into planar lipid bilayers (Morier and Sauve, 1994).

Voltage-sensitive gating of the Jurkat nuclear chloride channel

During the course of our experiments we noticed that the open probability of the Jurkat anion channel decreased as the pipette potential was made more negative (hyperpolarized). Fig. 5 *A* shows that after a 20-mV hyperpolarizing shift in pipette potential, the channel remained open for a few milliseconds, then inactivated. This is evidenced by an initial increase in single-channel amplitude (*dotted lines*) preceding channel closing. It is also evident that overall channel inactivation was greatest at strongly negative voltages. Fig. 5 *B* shows channel open probability (*NP*o) as a function of pipette potential, showing that channel closing is most marked below −80 mV. This effect of voltage is also apparent from monitoring of the voltage at which the channel first becomes inactivated. In the recording shown in Fig. 5 *C*, the pipette potential was first held at 0 mV and then jumped to voltages between −40 mV and −100 mV. In response to voltage steps to −40 mV or −60 mV, channel activity persisted for many minutes without closing. In contrast, a voltage jump to −80 mV resulted in channel activity that rapidly inactivated after ~20 s; at −100 mV the channel closed within 5 s. The effect of membrane potential was independent of the sequence in which the voltage pulses were given and was highly reproducible during a given recording. In symmetrical KCl (see Fig. 3 *A*), the channel open probability was largely invariant between +20 mV and +100 mV (data not shown).

Second-messenger modulation of a Jurkat nuclear chloride channel

The Jurkat anion channels could be consistently inhibited by nucleotides. Fig. 6 *A* shows a nucleus-attached recording where the simultaneous activities of four channels could be observed under resting conditions. Channel activity was inhibited within 2 min of the addition of GTPγS (20 μM; *arrow*) to the bath and was most pronounced within 3 min. However, the effect was only transient, as baseline activity returned to normal ~5 min after the addition of GTPγS. Fig. 6 *B* shows cumulative channel open probability (*NP*o) as a function of time for the recording interval shown in Fig. 6 *A*. Channel activity decreased from that of four simultaneously open channels to that of two channels or less. This effect is more clearly shown by utilizing amplitude histograms derived from periods before (Fig. 6 *C, top*), during (Fig. 6 *C, middle*), and after (Fig. 6 *C, bottom*) the effect of GTPγS. A transient effect of GTPγS was also observed in two other experiments with similar results (data not shown). These experiments suggest that the activity of the Jurkat chloride channel is modulated by G-protein-dependent mechanisms.

Nuclear anion channel activity on nuclear membranes (Tabares et al., 1991) and in bilayers (Rousseau et al., 1996) is inhibited by ATP. Characteristic features of the inhibition by ATP included concomitant reductions in single-channel amplitude and channel open probability. These features are also apparent in our nuclear recordings after the addition of ATP to the bath ($n = 3$). Fig. 6 *D* shows amplitude histograms generated before and after the addition of 2 mM ATP to the bath. Whereas the inhibition of channel activity with GTPγS required ~2 min to develop, the inhibition of channel activity with ATP was immediate. This could be interpreted to mean that ATP acts extranuclearly, while GTPγS may need to enter the perinuclear space to exert its effect. The transient nature of the effects of GTPγS and ATP may also reflect enzymatic activity present in the intact nuclei, because both agents persisted in the bath for the duration of the experiment (cf. Tabares et al., 1991; Rousseau et al., 1996). But dibutyryl-cAMP (50 μM) had no effect on channel activity when added to the bath for a duration of 8 min (data not shown).

Cation-selective channel expression in FL5 nuclei

We also examined ion channel activity of intact nuclei of FL5 cells. In contrast to the Jurkat T-cell line, the FL5

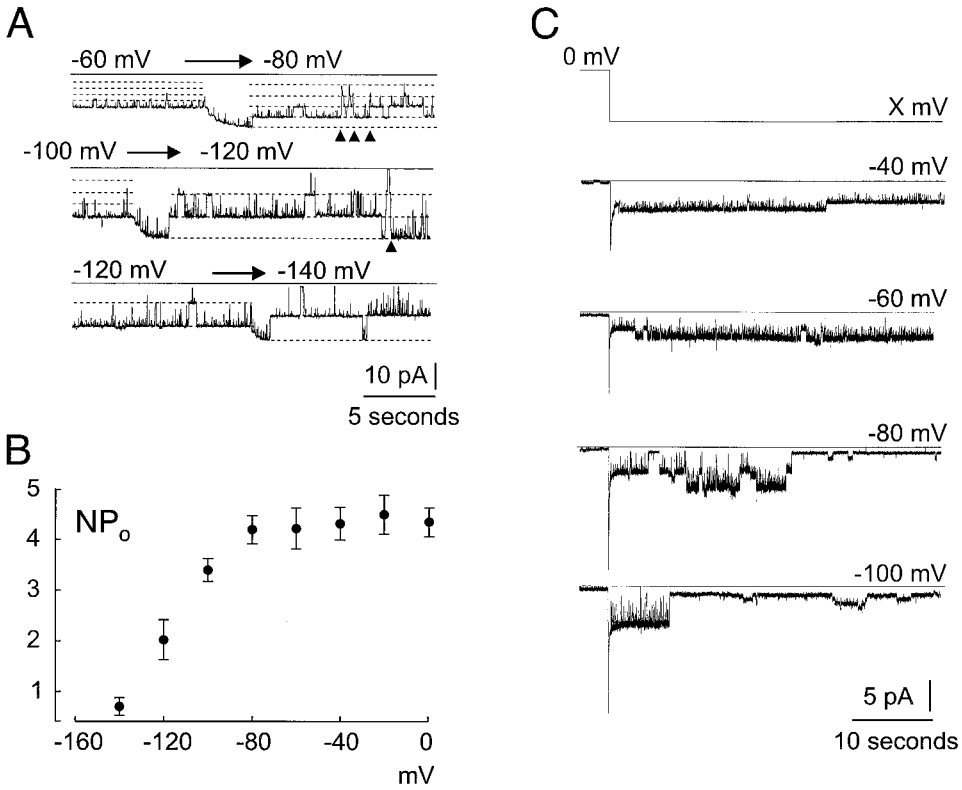

FIGURE 5 Voltage-sensitive gating of the Jurkat anion channel. (*A*) Channel closing in response to 20-mV hyperpolarization of the patch potential at the indicated patch potential. The solid and dotted lines indicate the 0 and open channel current levels, respectively. The horizontal arrows depict a ramp change in holding potential. The arrowheads indicate double-barreled openings. Current records were filtered at 50 Hz and sampled at 200 Hz. Current records were filtered more heavily to resolve channel transitions. (*B*) Channel open probability (NP_o) as a function of pipette potential. The data represent the mean of 5-s intervals for a 40-s recording duration at each potential. The relatively small standard deviations (± SD) indicate that channel activity was largely invariant during the interval measured. (*C*) Time to channel closing as a function of pipette potential. The pipette was held at 0 mV for ~1 min and next stepped to the indicated pipette potentials. This recording also shows the expression of a smaller conductance channel frequently observed at strongly negative pipette potentials. The solid lines indicate the 0 current level. Current records were filtered at 200 Hz and sampled at 1 kHz.

B-cell nuclei exhibited primarily cation-selective channels. With 150 K-aspartate in the bath and 150 KCl in the recording pipette, clear outward currents were observed over a broad range of positive pipette potentials beginning near 0 mV (Fig. 7 *A*). This contrasts sharply with the situation in Jurkat nuclei, where no outward currents were recorded with K-aspartate in the bath. The cumulative current-voltage relationship for several FL5 recordings is shown in Fig. 7 *B*. The mean outward slope conductance for these channels was 52 ± 2 pS (± SEM, $n = 16$), measured between +40 and +80 mV. The single-channel current reversed at 0 mV, suggesting cation (K^+) permeability. The cation permeability of these channels was further demonstrated by replacing extranuclear aspartate with equimolar (150 mM) chloride and showing that the reversal potential of the channel was not altered (Fig. 7 *C*; compare with Fig. 3, *C* and *D*). On the other hand, replacing the electrode solution with 100 mM $CaCl_2$ revealed no clear outward currents over a broad range of positive pipette potentials (data not shown). This might be taken to indicate an absence of divalent permeability or that the single-channel conductance was outside of detection. Such cation channels were in apparent in 20 of 22 on-nucleus patches from FL5 nuclei.

Voltage-sensitive gating of FL5 cation channel

The voltage dependence of the FL5 nuclear cation channel was opposite that observed for the Jurkat nuclear chloride channel. Channel activity was highest near 0 mV and decreased at more positive pipette potentials (see Fig. 7, *top traces*). Fig. 8 *A* shows representative current records, where it is apparent that channel activity was greater at +20 mV relative to +100 mV. Histograms of channel open times generated from recordings made at +20 mV and +100 mV are shown in Fig. 8 *B*. The histograms of channel open times were best fit by a sum of two exponentials. The faster component of the distribution typically had a time constant of ~1 ms, regardless of pipette potential (data not shown). Because this rapid component of open times was voltage

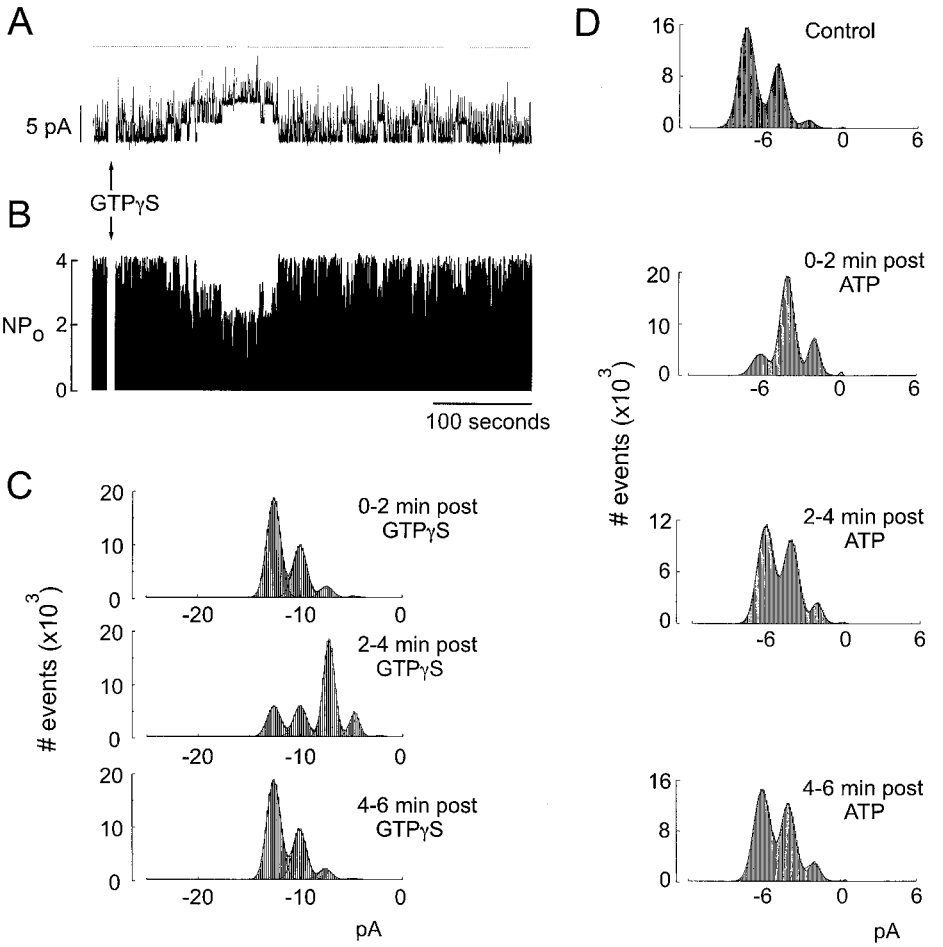

FIGURE 6 Transient inhibition of the anion channel in Jurkat nuclei by GTPγS and ATP. (*A*) An on-nucleus patch containing about four channels before and after the addition of 20 μM GTPγS (*arrow*). (*B*) Modifications in the channel open probability before and after the addition of GTPγS to the bath on a time base corresponding to that in *A*. (*C*) Amplitude histograms compiled from 2 min of recording at the indicated times after the addition of GTPγS. Dashed lines represent the 0 current level. Records were filtered at 20 Hz and sampled at 100 Hz. (*D*) Amplitude histograms compiled from 2 min of recording before and after the addition of 2 mM ATP at the indicated times. Note that both the single-channel amplitude and overall channel activity were transiently reduced by the addition of ATP. Both GTPγS and ATP were added to the bath for the duration of the experiment.

insensitive it was not examined further. The mean time constant of the slower component of the open time histogram increased from 2 ms at +20 mV to 6.6 ms at +100 mV. The cumulative histogram of mean channel open times is shown in Fig. 8 *C*; it shows that channel open times declined from ~6 ms at +100 mV to ~2 ms at +20 mV (*filled circles*). The empty circles correspond to the recording depicted in Fig. 7 *A* and show that channel open probability similarly decreases monotonically as the pipette potential is made more negative.

Anion-selective channel expression in FL5 nuclei

Anion channel activity like that characteristic of Jurkat nuclear recordings was sometimes observed in FL5 nuclear patches. Fig. 9 shows multichannel current-voltage relationships generated in response to voltage ramps from −140 mV to +140 mV. Fig. 9 *A* is the current response from an on-nucleus patch from a Jurkat cell to a ramp of voltage. For comparison, a similar voltage protocol was applied to a nuclear patch recording containing an anion channel from the surface of an FL5 nucleus (Fig. 9 *B*). The *I*/*V* relationship reveals features consistent with the chloride currents recorded from Jurkat nuclei, such as inward rectification and a positive reversal potential. Fig. 9 *C* shows the current response to a voltage ramp applied to another FL5 nuclear patch containing a cation channel. Cation selectivity in Fig. 9 *C* is indicated by the appearance of prominent outward currents at positive pipette potentials and current reversal at 0 mV. The "flickery" openings characteristic of the FL5 cation channels were also clearly observed. Cation channels like those observed in FL5 nuclei were never observed in recordings from Jurkat nuclei.

Larger conductance nuclear channels

We occasionally observed larger conductance, voltage-insensitive channel openings (data not shown). These channels had multiple conducting states of 50, 350, and 500 pS and were seemingly nonselective. The appearance of the large-conductance channels was not influenced by excising the patch from the nuclear surface and was equally infrequent in both cell types (~5% of all recordings). Based on physical dimensions, the conductance of the fully open

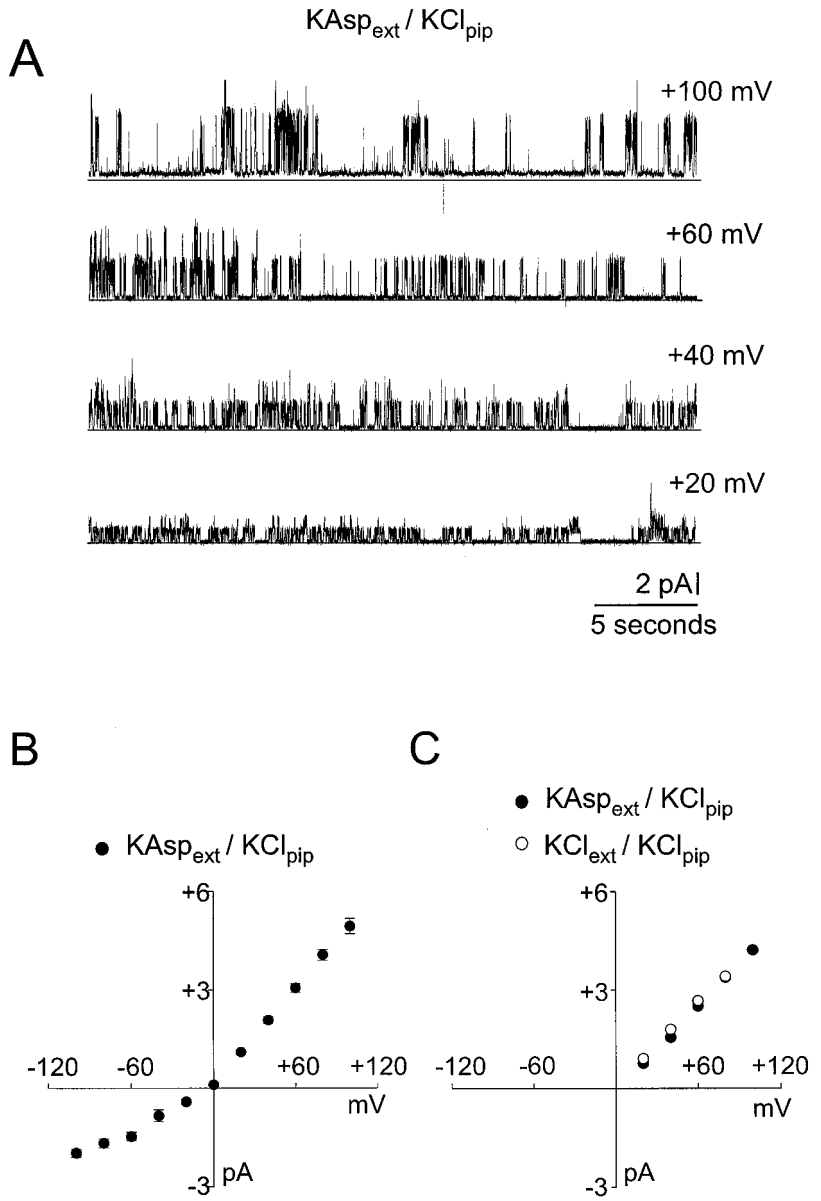

FIGURE 7 Cation selectivity of nuclear channels derived form FL5 cells. (*A*) Single-channel current traces at the indicated patch potential with K-aspartate (150 mM) in the bath and KCl in the electrode (150 mM). The solid lines represent the 0 current level. (*B*) Mean current-voltage relationship for channel currents recorded from FL5 nuclei. Each symbol represents the mean of 10–14 measurements. The mean outward slope conductance for such channels was 52 ± 2 pS (n = 16, ± SEM) calculated between +40 and +80 mV. (*C*) Replacing 150 mM K-aspartate in the bath with 150 mM KCl did not alter the single-channel amplitude. Open circles represent current amplitudes made in the presence of symmetrical KCl. The single-channel slope conductance in extranuclear KCl and K-aspartate was 48 and 42 pS, respectively. The solid lines indicate the 0 current level. The current records were sampled at 1 kHz and filtered at 200 Hz.

nuclear pore has been estimated to be ~1 nS (Mazzanti et al., 1990), and some have proposed that the nuclear pore opens in conductance increments of 300 pS, consistent with these large openings (Tonini et al., 1999). However, the proposed large conductance and apparent abundance of nuclear pores make it unlikely that they correspond to the frequently observed ion-selective channels measured in patch clamp here (see Fig. 2). Furthermore, despite the fact that nuclear pores were consistently observed at roughly similar densities in both Jurkat and FL5 nuclei by atomic force microscopy, nuclear channel activity differed dramatically between the two cell lines. Again this suggests that the channels are not nuclear pores, but rather are ion channels like those common in the plasma membrane. We propose that the nuclear pores were mainly nonconducting under our recording conditions, perhaps because of our Ca^{2+}-free solutions or the washout of cytosolic mediators (cf. Perez-Terzic et al., 1997).

DISCUSSION

Comparison with other studies

The main finding of this study is that the ion channels on the outer nuclear envelopes of B- and T-cell lines are distinctly different. In T-cell nuclei, the channels are primarily anion selective, while in B cells they are cation selective. Although the functional significance of this finding is currently not understood and may be the result of the transformation process or clonal selection of the cell lines, it is

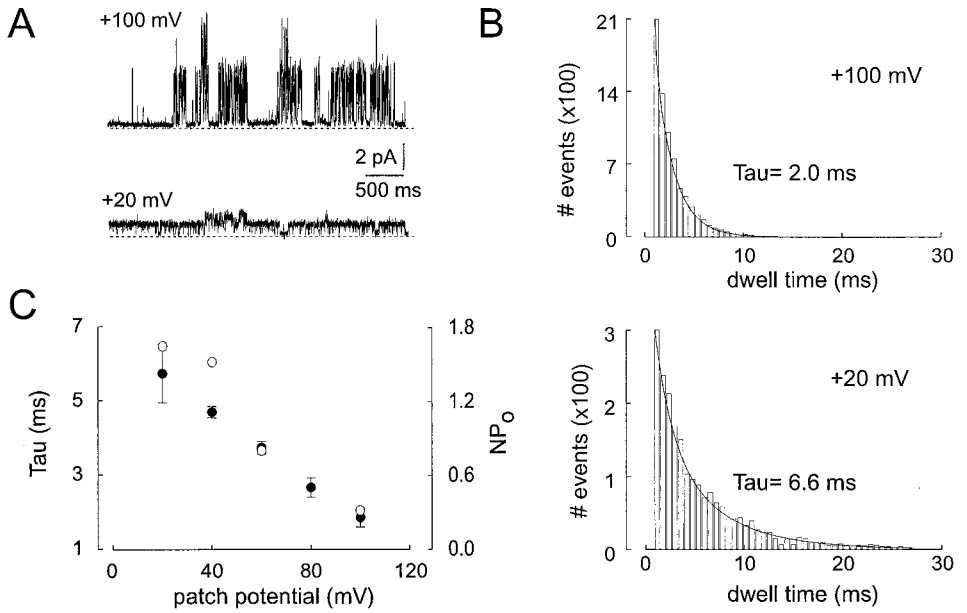

FIGURE 8 Voltage-dependent gating of nuclear FL5 cation channels. (*A*) Representative current records at the indicated patch potentials. Records were sampled at 2 kHz and filtered at 500 Hz. Dashed lines represent the 0 current level. (*B*) Histograms of channel open times at the indicated patch potentials. Histograms were generated from current records sampled at 5 kHz and filtered at 1 kHz. (*C*) Mean channel open time as a function of patch potential (*filled circles*). Each point represents the average of four to six measurements (± SD). The empty circles correspond to the recording shown in Fig. 7 *A* and show that channel open probability likewise decreases at positive pipette potentials. Mean channel open probability was calculated from 20–40 s of recorded channel activity.

nevertheless intriguing to speculate on the biological implications of ion channel diversity in the nuclear envelope. This is especially true if we assume that such channels contribute to the sequestration of cytosolic calcium in cellular organelles. For example, nuclear channel diversity may be manifested as differences in sensitivity of gene expression to nucleo/cytoplasmic calcium signaling. In this respect, cytosolic calcium increments of different amplitudes and durations have been shown to differentially modulate gene transcription in Jurkat cells (Dolmetsch et al., 1997). Furthermore, some aspects of apoptosis are thought to be either assisted or averted by the expression of anionic (BAX) or cationic (Bcl-2, Bcl-xl) ion channels of the BCl-2 superfamily, respectively, on the nuclear envelope, endoplasmic reticulum, or mitochondrial membrane (Schendel et al., 1998). These are known sites of calcium sequestration for the cell. In light of these findings it is important to note that Bcl-2 overexpression alters intracellular calcium handling in lymphoma cells (He et al., 1997). Finally, we have preliminary data showing that overexpression of Bcl-xl apparently attenuates nuclear channel activity in Jurkats but not FL5s. However, whether this is a pleiotropic effect of averted programmed cell death or is actually due to ion incorporation into the nuclear envelope is unresolved.

Several classes of nuclear ion channels have been described in distinct cell types and species (reviewed by Stehno-Bittel et al., 1996). Anionic channels of 150 and 58 pS (hepatocytes; Tabares et al., 1991) and 150 pS (cardiac myocytes; Rousseau et al., 1996) have been measured. Cationic channels have also been reported with conductances of 166 pS (neurons; Draguhn et al., 1997), 180 pS (cardiac myocytes; Rousseau et al., 1996), 200 pS (pancreatic acinar cells; Maruyama et al., 1995), 200 pS (mammalian pronuclei; Mazzanti et al., 1990), 106–532 pS (cardiac myocytes; Bustamante, 1992) and 800 pS (erythrocytes; Matzke et al., 1990). Large-conductance nuclear channels of unresolved selectivity have also been reported (e.g., 50–1000 pS, *Xenopus* oocytes, Mazzanti et al., 1994; and 200-1700 pS, hepatocytes, Assandri and Mazzanti, 1997). Despite the fact that a wide diversity of nuclear ion channels has been described in the literature, their function, as yet, remains largely speculative.

Heterogeneous ion channel expression has also been reported between the inner and outer nuclear envelopes (Rousseau et al., 1996). Rousseau et al. found that large-conductance chloride channels (150 pS; 50/250 mM KCl *trans*/*cis* in bilayers) were more common on the outer nuclear envelope than on the inner nuclear envelope. The voltage dependence and appearance of multiple conducting states for these channels were similar to those of the Jurkat nuclear chloride channels reported here. Moreover, the density of the 150-pS chloride channel in bilayers was calculated to be $\sim 10/\mu m^2$, roughly the same as the density we observed in Jurkat nuclear recordings. These authors observed cation-selective channels on the outer nuclear envelope but not on the inner envelope. However, these channels were unlike the cation channels we observed on FL5 nuclei, with the bilayer channels having a much larger single-channel conductance (~180 pS) and distinct gating kinetics. Interestingly, the differences in the voltage dependence of the 150-pS chloride and 180-pS cation channels observed in bilayers were paralleled by the 80-pS chloride and 50-pS cationic nuclear channels described in this report.

Jurkat nuclear anion channels

The elevated channel activity of the Jurkat anion channels complicated the analysis of their gating. Typically more

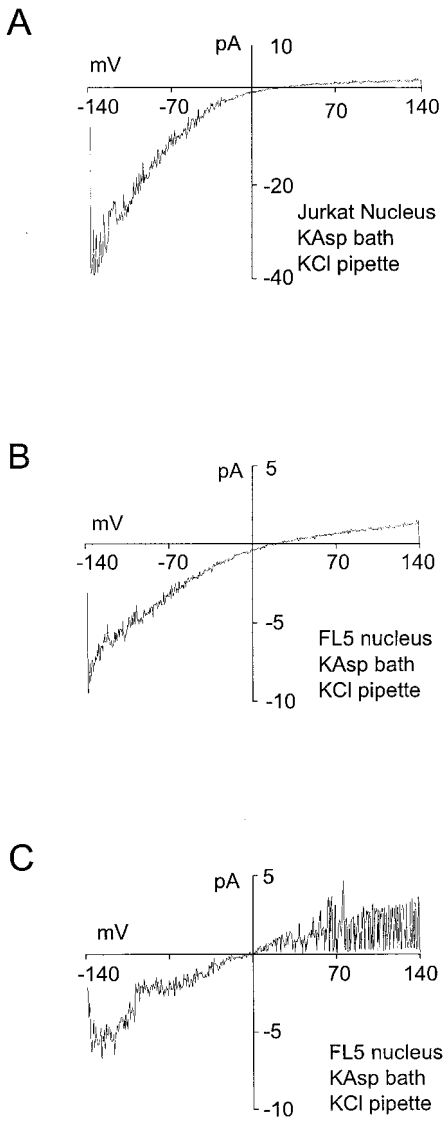

FIGURE 9 Macroscopic currents elicited with voltage ramps. Voltage ramps from −140 mV to +140 mV were applied to nuclei-attached patches for a duration of 4 s. (*A*) Voltage ramp applied to a Jurkat nucleus demonstrating characteristic, inwardly rectifying, anion channel activity. (*B* and *C*) Voltage ramps applied to FL5 nuclear patches demonstrating anion-selective (*B*) and cation-selective (*C*) conductances. The current records were sampled at 5 kHz and filtered at 1 kHz. The recording conditions are given in the figure.

than six conductance levels were observed per nuclear patch, making it difficult to fully discern the double-barreled gating characteristics of the channels. Therefore, the conductance measurements presented in Fig. 3 most likely correspond to the opening of only a single protopore of the homodimeric channel and underestimate the conductance of the fully open channel by half. Elevated "resting" open probability could result from peculiarities of our recording conditions, for example, the absence of perinuclear Ca^{2+} or other modulatory second messengers lost during nuclear isolation.

The single-channel conductance at negative pipette potentials is smaller in the presence of extranuclear (outside the pipette) K-aspartate. Under such conditions the electrochemical driving force on chloride is actually larger and channel currents should have increased in accordance. The simplest explanation for this is that extranuclear aspartate (or gluconate) may be either blocking (or permeating at a very low rate) the channel from the inside. Aspartate and gluconate seem to be equally impermeable. Although quantitative arguments comparing reversal potentials cannot be made because of the strong rectification of the current-voltage relationship, this result also agrees with the fact that the apparent reversal potential in the presence of aspartate (or gluconate; $\sim +20$ mV) is less positive than expected if the channel where permeable solely to chloride ($\sim +70$ mV).

Inward rectification also appears to be an inherent property of the anion channel because it persists in excised patches in the presence of symmetrical chloride, largely independent of the chloride gradient. With respect to the cytoplasm, an inwardly rectifying anion current on the nuclear envelope compares to an outwardly rectifying anion current on the plasma membrane. Interestingly, ClC-5 gives rise to a plasma membrane current that is both outwardly rectifying and inhibited by low pH (Friedrich et al., 1999). In addition, expression of ClC-6 in *Xenopus* oocytes gives rise to membrane currents that are outwardly rectifying as well as slowly inactivated by membrane potentials greater than +60 mV (< -60 mV in our recording system; also see our Fig. 5; Buyse et al., 1997). Finally, rat brain endothelial cells express an endogenous chloride current that is outwardly rectifying, inactivated by membrane voltages greater than +80 mV, and inhibited by extracellular ATP (10 mM; von Weikersthal et al., 1999). The endothelial cell current was activated by hypotonic cell swelling and was proposed to arise from the expression of ClC-3 on the cell surface, although ClC-2 and ClC-5 were also present in those cells. The striking similarities in gating kinetics, voltage dependency, and pharmacology observed between members of the ClC superfamily and the anion channels described here support our conclusion that we are in fact monitoring the activity of an intracellular ClC homolog on the nuclear envelope.

Intracellular ClC homologs

Several ClC homologs have been proposed to function intracellularly. *GEF1* is a yeast respiratory mutant deficient in nonfermentable substrate utilization (Greene et al., 1993). The *GEF1* gene has been cloned and shown to encode a novel member of the ClC chloride channel superfamily. It is thought that the *GEF1* channel, by maintaining electroneutrality, permits the loading of Cu^{2+}, a necessary cofactor in

yeast respiration, into post-Golgi respiratory vesicles (Gaxiola et al., 1998). Mutations in intracellular ClC homologs have also been implicated in human genetic disorders. Dent's disease, an X-linked human disorder characterized by low-molecular-weight proteinuria, hypercalciuria, and kidney stones (Wrong et al., 1994), results from a defect in the *ClC-5* gene (Lloyd et al., 1996). Recently, Gunther et al. (1998) have shown that ClC-5 colocalizes with the proton ATPase of endocytotic vesicles, where it is thought to provide an electrical shunt permitting vesicle acidification. A defect in endosome-mediated uptake could account for the low-molecular-weight proteinuria characteristic of Dent's disease.

ClC-2 is associated with intracellular zymogen granules of pancreatic acinar cells (Carew and Thorn, 1996). These channels may appear transiently on the cell membrane after exocytosis because membrane chloride currents can be recorded from these cells. It has been proposed that ClC-2 chloride fluxes mediate vesicle swelling before fusion. Therefore, four members of the ClC family (GEF1, ClC-6, ClC-5, and ClC-2) may function intracellularly. Although reverse transcriptase-polymerase chain reaction has demonstrated the existence of ClC-6 splice variants in Jurkat nuclei (data not shown; see also Eggermont et al., 1997), the molecular identity of the ClC homolog on T-cell nuclear membrane is unknown.

Nuclear cation channels in FL5 cells

Overall channel activity was less in FL5 nuclei compared to Jurkat nuclei. On average there were 2 ± 0.5 ($\pm$ SD; $n = 18$) channels per on-nucleus patch from recording on FL5 nuclei. In addition, whereas Jurkat nuclei exhibited only anion channels, both anion and cation channels were observed on FL5 nuclei. As a result the "inward" currents in the negative voltage range were often contaminated with other channel types in FL5 nuclei, including the inward rectifying chloride channel. Finally, assuming that the perinuclear stores were depleted in the absence of extranuclear Ca^{2+} (5 mM EGTA in the bath), these channels are not the Ca^{2+}-activated potassium channels previously described in heart sarcoplasmic reticulum (Uehara et al., 1994), tracheal endoplasmic reticulum and secretory vesicles (Nguyen et al., 1998), or the pancreatic acinar nuclear envelope (Maruyama et al., 1995). Unlike the anion channels observed in Jurkat nuclei, GTPγS did not influence the activity of the cation channels. Therefore, the channels are probably not the G-protein-regulated potassium channels previously described in chromaffin granule membranes (cf. Arispe et al., 1995).

Our results demonstrate that the nuclear envelope of T- and B-cell cell lines expresses different ion channel classes with differing selectivities, voltage-sensitive gating mechanisms, and pharmacological sensitivities. In the future it would be important to determine if these differences also extend to nontransformed lymphocytes. Nonetheless, these differences in channel characteristics may reflect currently unknown functions of the nuclear envelope.

We thank Aron Shapiro for excellent technical assistance in the preparation of nuclei preparations. We also acknowledge Dr. Michael N. Badminton, who conducted the confocal microscopic experiment depicted in Fig. 2.

REFERENCES

Al-Awqati, Q. 1995. Chloride channels of intracellular organelles. *Curr. Opin. Cell Biol.* 7:504–508.

Arispe, N., P. DeMazancourt, and E. Rojas. 1995. Direct control of a large conductance K^+-selective channel by G-proteins in adrenal chromaffin granule membranes. *J. Membr. Biol.* 147:109–119.

Assandri, R., and M. Mazzanti. 1997. Ionic permeability on isolated mouse liver nuclei: influence of ATP and Ca^{2+}. *J. Membr. Biol.* 157:301–309.

Brandt, S., and T. J. Jentsch. 1995. ClC-6 and ClC-7 are two novel broadly expressed members of the ClC chloride channel family. *FEBS Lett.* 377:15–20.

Bustamante, J. O. 1992. Nuclear ion channels in cardiac myocytes. *Pflugers Arch.* 421:473–485.

Buyse, G., D. Trouet, T. Voets, L. Missiaen, G. Droogmans, B. Nilius, and J. Eggermont. 1998. Evidence for the intracellular location of chloride channel (ClC)-type proteins: co-localization of ClC-6a and ClC-6c with the sarco/endoplasmic-reticulum Ca^{2+} pump SERCA2b. *Biochem. J.* 330:1015–1021.

Buyse, G., T. Voets, J. Tytgat, C. DeGreef, G. Droogmans, B. Nilius, and J. Eggermont. 1997. Expression of human pI_{Cln} and ClC-6 in *Xenopus* oocytes induces an identical endogenous chloride conductance. *J. Biol. Chem.* 272:3615–3621.

Carew, M., and P. Thorn. 1996. Identification of ClC-2-like chloride currents in pig pancreatic acinar cells. *Pflugers Arch.* 433:84–90.

Clark, A. G., D. Murray, and R. H. Ashley. 1997. Single channel properties of a rat brain endoplasmic reticulum anion channel. *Biophys. J.* 73: 168–178.

Danker, T., M. Mazzanti, R. Tonini, A. Rakowska, and H. Oberleithner. 1997. Using atomic force microscopy to investigate patch-clamped nuclear membrane. *Cell Biol. Int.* 21:747–757.

Divecha, N., H. Banfic, and R. F. Irvine. 1993. Inositides and the nucleus and inositides in the nucleus. *Cell.* 74:405–407.

Dolmetsch, R. E., R. S. Lewis, C. C. Goodnow, and J. I. Healy. 1997. Differential activation of transcription factors induced by Ca^{2+} response amplitude and duration. *Nature.* 386:855–858.

Draguhn, A., G. Borner, R. Beckmann, K. Buckner, U. Heinemann, and F. Hucho. 1997. Large-conductance cation channels in the envelope of nuclei from rat cerebral cortex. *J. Membr. Biol.* 158:159–166.

Duncan, R. R., P. K. Westwood, A. Boyd, and R. H. Ashley. 1997. Rat brain p64H1, expression of a new member of the p64 chloride channel protein family in the endoplasmic reticulum. *J. Biol. Chem.* 272: 23880–23886.

Edwards, J. C., B. Tulk, and P. H. Schlesinger. 1998. Functional expression of p64, an intracellular chloride channel protein. *J. Membr. Biol.* 163: 119–127.

Eggermont, J., G. Buyse, T. Voets, J. Tytgat, H. DeSmedt, G. Droogmans, and B. Nilius. 1997. Alternative splicing of ClC-6 (a member of the ClC chloride-channel family) transcripts generated three truncated isoforms one of which, ClC-6c, is kidney-specific. *Biochem. J.* 325:269–276.

Eliassi, A., L. Garneau, G. Roy, and R. Sauve. 1997. Characterization of a chloride-selective channel from rough endoplasmic reticulum membranes of rat hepatocytes: evidence for a block by phosphate. *J. Membr. Biol.* 159:219–229.

Franco-Obregón, A., and D. E. Clapham. 1998. Distinct ion channel classes expressed on the outer nuclear membrane of T and B cell lymphocytes as revealed using the patch clamp technique. *In* 52nd Annual Meeting of

the Society of General Physiologists. Rockefeller University Press, New York. 104.

Friedrich, T., T. Briederhoff, and T. Jentsch. 1999. Mutational analysis discriminates that ClC-4 and ClC-5 directly mediate plasma membrane currents. *J. Biol. Chem.* 274:896–902.

Gaxiola, R. A., D. S. Yuan, R. D. Klausner, and G. R. Fink. 1998. The yeast ClC chloride channel functions in cation homeostasis. *Proc. Natl. Acad. Sci. USA.* 95:4046–4050.

Gerasimenko, O. V., J. V. Geraskimenko, A. V. Tepikin, and O. H. Petersen. 1995. ATP-dependent accumulation and inositol triphosphate- or cyclic ADP-ribose-mediated release of Ca^{2+} from the nuclear envelope. *Cell.* 80:439–444.

Gilchrist, J. S., and G. N. Pierce. 1993. Identification and purification of a calcium-binding protein in hepatic nuclear membranes. *J. Biol. Chem.* 268:4291–4299.

Gorlich, D. 1988. Transport into and out of the nucleus. *EMBO J.* 17: 2721–2727.

Greene, J. R., N. H. Brown, B. J. DiDomenico, J. Kaplan, and D. J. Eide. 1993. The *GEF1* gene of *Saccharomyces cerevisiae* encodes an integral membrane protein: mutations in which have effects on respiration and iron-limited growth. *Mol. Gen. Genet.* 241:542–553.

Guihard, G., S. Proteau, and E. Rousseau. 1997. Does the nuclear envelope contain two types of ligand-gated Ca^{2+} release channels? *FEBS Lett.* 414:89–94.

Gunther, W., A. Luchow, F. Cluzeaud, A. Vandewalle, and T. Jentsch. 1998. ClC-5, the chloride channel mutated in Dent's disease, colocalizes with the proton pump in endocytotically active kidney cells. *Proc. Natl. Acad. Sci. USA.* 95:8075–8080.

He, H., M. Lam, T. S. McCormick, and C. W. Distelhorst. 1997. Maintenance of calcium homeostasis in the endoplasmic reticulum by Bcl-2. *J. Cell. Biol.* 138:1219–1228.

Hennager, D. J., M. J. Welsh, and S. DeLisle. 1995. Changes in either cytosolic or nucleoplasmic inositol 1,4,5-triphosphate levels can control nuclear Ca^{2+} concentration. *J. Biol. Chem.* 270:4959–4962.

Humbert, J., N. Matter, J. Artault, P. Koppler, and A. Malviya. 1996. Inositol 1,4,5-triphosphate receptor is located to the inner nuclear membrane vindicating regulation of nuclear calcium signaling by inositol 1,4,5-triphosphate. *J. Biol. Chem.* 270:478–485.

Landry, D., S. Sullivan, M. Nicolaides, C. Redhead, A. Edelman, M. Field, Q. Al-Awqati, and J. Edwards. 1993. Molecular cloning and characterization of p64, a chloride channel protein from kidney microsomes. *J. Biol. Chem.* 268:14948–14955.

Lanini, L., O. Bachs, and E. Carafoli. 1992. The calcium pump of the liver nuclear membranes is identical to that of the endoplasmic reticulum. *J. Biol. Chem.* 267:11548–11552.

Lipp, P., D. Thomas, M. J. Berridge, and M. D. Bootman. 1997. Nuclear calcium signalling by individual cytoplasmic calcium puffs. *EMBO J.* 16:7166–7173.

Lloyd, S. E., S. H. S. Pearce, S. E. Fisher, S. J. Steinmeyer, B. Schwappach, S. J. Scheinman, B. Harding, A. Bolino, M. Devoto, P. Goodyear, S. P. A. Rigden, O. Wrong, T. J. Jentsch, I. W. Craig, and R. V. Thakker. 1996. A common molecular basis for three inherited kidney stone diseases. *Nature.* 379:445–449.

Maruyama, Y., H. Shimada, and J. Taniguchi. 1995. Ca^{2+} activated K^+ channels in the nuclear envelope from single pancreatic acinar cells. *Pflugers Arch.* 430:148–150.

Matzke, A. J. M., T. M. Weiger, and M. A. Matzke. 1990. Detection of a large cation-selective channel in nuclear envelopes of avian erythrocytes. *FEBS Lett.* 271:161–164.

Mazzanti, M. 1998. Ion permeability of the nuclear envelope. *News Physiol. Sci.* 13:44–50.

Mazzanti, M., L. J. DeFelice, J. Cohen, and H. Malter. 1990. Ion channels in the nuclear envelope. *Nature* 343:764–767.

Mazzanti, M., B. Innocenti, and M. Rigatelli. 1994. ATP ionic permeability on the nuclear envelope in situ nuclei of Xenopus oocytes. *FASEB J.* 8:231–236.

Miller, C., and M. M. White. 1984. Dimeric structure of single chloride channels from *Torpedo electroplax*. *Proc. Natl. Acad. Sci. USA.* 81: 2772–2775.

Morier, N., and R. Sauve. 1994. Analysis of a novel double-barreled anion channel from rat liver rough endoplasmic reticulum. *Biophys. J.* 67: 590–602.

Nguyen, T., W. Chin, and P. Verdugo. 1998. Role of Ca^{2+}/K^+ ion exchange in intracellular storage and release of Ca^{2+}. *Nature.* 395: 908–912.

Perez-Terzic, C., M. Jaconi, and D. E. Clapham. 1997. Nuclear calcium and the regulation of the nuclear pore complex. *Bioessays.* 19:787–792.

Petersen, O. H., O. V. Gerasimenko, J. U. Gerasimenko, H. Mogami, and A. V. Tepikin. 1998. The calcium store in the nuclear envelope. *Cell Calcium.* 23:87–90.

Pollock, N. S., M. E. Kargacin, and G. J. Kargacin. 1998. Chloride channel blockers inhibit Ca^{2+} uptake by smooth muscle sarcoplasmic reticulum. *Biophys. J.* 75:1759–1766.

Rousseau, E., C. Michaud, D. Lefebvre, S. Proteau, and A. Decrouy. 1996. Reconstitution of ionic channels from inner and outer membranes of mammalian cardiac nuclei. *Biophys. J.* 70:703–714.

Schendel, S. L., M. Montal, and J. C. Reed. 1998. Bcl-2 family proteins as ion-channels. *Cell. Death Differ.* 5:372–380.

Stehno-Bittel, L., A. Luckhoff, and D. E. Clapham. 1995a. Calcium release from the nucleus by IP_3 receptor channels. *Neuron.* 14:163–167.

Stehno-Bittel, L., C. M. Perez, and D. E. Clapham. 1995b. Nuclear Ca^{2+} store regulates diffusion across the nuclear envelope. *Science.* 270: 1835–1838.

Stehno-Bittel, L., C. Perez-Terzic, A. Luckhoff, and D. E. Clapham. 1996. Nuclear ion channels and regulation of the nuclear pore. *In* Organellar Ion Channels and Transporters, Vol. 51. Society of General Physiologists. D. E. Clapham and B. E. Ehrlich, editors. Rockefeller University Press, New York. 195–207.

Subramanian, K., and T. Meyer. 1997. Calcium-induced restructuring of the nuclear envelope and endoplasmic reticulum calcium stores. *Cell.* 89:963–971.

Tabares, L., M. Mazzanti, and D. E. Clapham. 1991. Chloride channels in the nuclear membrane. *J. Membr. Biol.* 123:49–54.

Tonini, R., F. Grohovaz, C. A. M. Laporta, and M. Mazzanti. 1999. Gating mechanism of the nuclear pore complex channel in isolated neonatal and mouse liver nuclei. *FASEB J.* 13:1395–1403.

Uehara, A., M. Yasukochi, and I. Imanaga. 1994. Calcium modulation of single SR potassium channel currents in heart muscle. *J. Mol. Cell Cardiol.* 26:195–202.

Valenzuela, S. M., D. K. Martin, S. B. Por, J. M. Robbins, K. Warton, M. R. Bootcov, P. R. Schofield, T. J. Campbell, and S. N. Breit. 1997. Molecular cloning and expression of a chloride ion channel of cell nuclei. *J. Biol. Chem.* 272:12575–12582.

von Weikersthal, S. F., M. A. Barrandand, and S. B. Hladky. 1999. Functional and molecular characterization of a volume-sensitive chloride current in rat brain epithelial cells. *J. Physiol. (Lond.).* 516.1:75–84.

Wang, H., and D. E. Clapham. 1999. Conformational changes of the in situ nuclear pore complex. *Biophys. J.* 77:241–247.

Weis, K. 1998. Importins and exportins: how to get in and out of the nucleus. *Trends Biochem. Sci.* 269:185–189.

Wrong, O., A. Norden, and T. G. Feest. 1994. Dent's disease; a familial proximal renal tubular syndrome with low-molecular-weight proteinuria, hypercalciuria, nephrocalcinosis, metabolic bone disease, progressive renal failure and a marked male predominance. *Q. J. Med.* 87: 473–493.